

## Ray Tracer Simulation of Si-Based Solar Cells using Al<sub>2</sub>O<sub>3</sub>/ITO as Double Layers Anti Reflective Coating

Nurul Aina Nabihah Hamdan<sup>1</sup>, Noorsyam Yusof<sup>1</sup> and Mohd Zaki Mohd Yusoff<sup>2,\*</sup>

<sup>1</sup>Faculty of Applied Sciences, Universiti Teknologi MARA, Perlis 02600, Malaysia

<sup>2</sup>School of Physics and Material Studies, Faculty of Applied Sciences, Universiti Teknologi MARA, Selangor 40450, Malaysia

(\*Corresponding author's e-mail: [zaki7231@uitm.edu.my](mailto:zaki7231@uitm.edu.my))

Received: 6 September 2022, Revised: 7 October 2022, Accepted: 14 October 2022, Published: 1 June 2023

### Abstract

The solar cell has become one of the options for a greener world. Various studies have been done to achieve a solar cell with high efficiency and reasonable price. This study's objective is to investigate how the thickness and base angle of the front layer affect the optical and electrical characteristics of Si-Based Solar cells. To accomplish this study, heterojunction solar cells using Al<sub>2</sub>O<sub>3</sub>/ITO as the double layer anti-reflection coating are analyzed using the Wafer Ray Tracer simulation by the PV Lighthouse. Al<sub>2</sub>O<sub>3</sub> and ITO layers are used as a double anti-reflection coating (DLARC) in the light trapping strategy to support the reflection, absorption, and transmission (R, A and T) of the silicon solar cell. It acts to minimize reflectance and improves the overall efficiency of the solar cell. DLARC variation focuses on increasing absorption while decreasing reflection and transmission. The high refractive index of the hydrogenated a-Si (a-Si: H) emitter layer generates excessive reflection losses in SHJ solar cells making the silicon wafer have a low absorption efficiency. The DLARC thickness and base angle are varied as part of the simulation using the Wafer Ray Tracer by PV Lighthouse. The surface morphology of upright pyramid texture, height is 3.536 μm, texture base angle 54.74 °, and width 5 μm are used for reference scheme. Four schemes will be analyzed throughout this study along with the reference scheme. The result of this study is that Scheme 3 gives the optimum result with 99 % absorption, 21 % reflection and 67 % transmission. The goal of this study is to evaluate the impact of ARC thickness on optical and electrical characteristics. The best outcome is produced by varying the thickness and base angle of Scheme 3. The highest J<sub>max</sub> value, 0.3842 mA/cm<sup>2</sup>, is found in Scheme 3.

**Keywords:** Solar cell, Anti-reflection coating, ARC, Ray simulation, Photo-generation

### Introduction

Due to its promise of renewability and sustainability, solar energy is seen as an excellent replacement for traditional resources and is proliferating [1]. Using the photovoltaic effect, a photovoltaic (PV) or solar cell turns the energy of sunlight directly into electricity [2]. The photovoltaic effect results from the absorption of light radiation due to the photo generation of charge carriers in light-absorbing material. Electron-hole pairs are created by light irradiation, which then separated under bias to provide an electric potential [3]. PV cells have low efficiency and a high production cost, preventing them from being used on a broad scale. Using the Ray Tracer simulation, a textured surface of transparent conductive oxide (TCO) and a dielectric will be chosen as the anti-reflective coating. The silicon heterojunction (SHJ) solar cells rely on indium tin oxide (ITO) thin films, which serve as both an anti-reflection layer and a carrier transport layer in both the vertical and lateral orientations [4]. ITO film also has good electrical conductivity and can be used as an ohmic contact [5]. Beside, ITO electrode has a strong capacity for carrier collection [6]. The dielectric chosen is Al<sub>2</sub>O<sub>3</sub> has outstanding stability, high dielectric strength, resilience under harsh conditions and high transparency [7,8].

Crystalline silicon (c-Si) has been in the market with demand for over 90 % of production [9]. The high energy conversion efficiency potential (> 24 %) of SHJ solar cells is one of its main advantages [10]. SHJ solar cells with high efficiency are made by combining amorphous silicon (a-Si) and c-Si technologies [11]. Therefore, SHJ solar cells are also well-suited for thin c-Si wafer applications [12]. Optical losses must be lowered to improve the solar cell's absorption properties, which are critical for achieving high efficiency. Anti-reflection coating minimizes reflectance and improves the solar cell [13].

The inclusion of silicon on a dielectric thin film's surface boosts the cell's performance.  $\text{Al}_2\text{O}_3$  is a fascinating substance that can be used as an anti-reflection coating [13].  $\text{Al}_2\text{O}_3$  has a high refractive index and great transparency over a wide spectral range, which are its main advantages [13]. To minimize reflectance on a textured surface that is used to achieve proper light trapping and anti-reflection properties, TCO is used while enhancing photon infusion from the solar spectrum into the device [10]. TCO material used as the front film material in this project is ITO, which is also used as an anti-reflection coating.

Texturing (internal) device surfaces to scatter incident light away from the specular direction is a regularly used light management technique for increasing light absorption [14]. Surface texturing is used to improve the absorption of the silicon solar cell on top of using the anti-reflection coating. This study developed  $\text{Al}_2\text{O}_3/\text{ITO}$  DLARC with a thickness of 50/70 nm to reduce surface reflection and boost light absorption [7]. The  $\text{Al}_2\text{O}_3/\text{IZO}$  layer has a larger antireflective influence, which improves the optoelectronic capabilities, according to simulated studies [15].  $\text{Al}_2\text{O}_3/\text{IZO}$  films demonstrated better optical and electrical properties than single layers of ITO and IZO films thanks to their low reflectance of 2.2 % in the wavelength range of 300 - 1,100 nm [15]. Besides,  $\text{Al}_2\text{O}_3$  was used as an ARC layer for GaAs solar cells, yielding the greatest values of  $I_{sc} = 3.11$  A and  $V_{oc} = 0.884$  V [16]. Using the Essential Macleod Program and Crosslight APSYS software, the broadband graded refractive index  $\text{TiO}_2/\text{Al}_2\text{O}_3/\text{MgF}_2$  TLAR coating for the GaInP/InGaAs/Ge lattice-matched TJ solar cell has been studied [17]. The average reflectance of a TJ solar cell is decreased from 25.57 to 3.37 % thanks to TLAR coating, which has a stronger antireflection effect in the wavelength range of 300 - 1,800 nm than  $\text{TiO}_2/\text{Al}_2\text{O}_3$  DLAR coating [17]. Using optoelectrical simulations, Wang improved the structure of thin  $\text{Cu}(\text{In,Ga})\text{Se}_2$  (CIGS) solar cells with a grating aluminium oxide ( $\text{Al}_2\text{O}_3$ ) passivation layer (GAPL) offering nano-sized contact holes [18]. The efficient carrier recombination inhibition and high reflectivity of the  $\text{Al}_2\text{O}_3$  insulator passivation with local contacts caused the efficiency value to peak at 100 nm for the contact opening width [18].

Due to surface texturing on the front film, there will be an increase in the surface area where the absorption of sunlight occurs. Thus, the optical and electrical properties of heterojunction solar cell that consists of reflection, absorption and transmission can depend on the surface texturing on the front film that came in contact first with the sunlight. These findings benefit the front film's optical and electrical properties using  $\text{Al}_2\text{O}_3$  and ITO as a double-layer anti-reflective coating. The outcome of a thin layer must-have is high absorption, low transmission, and low reflection of the silicon wafer. The destructive interference of light reflected from the interfaces of the coating layers is the basis of single and multilayer antireflection coatings [19]. A double layer of anti-reflection coating is used due to limitations in the single layer anti-reflection coating. The number of materials with an appropriate index restricts the efficiency of a single-layer antireflection coating [19]. Furthermore, only 1 wavelength may achieve 0 or minimum reflectance, and the reflectance increases fast on both sides of the 0 or lowest position. These problems are largely solvable by employing coating that has 2 or more layers of ARC. This problem makes it possible to use the double layer anti-reflection coating than the single layer anti-reflection coating. This study is significant to current industrial solar cells as an affordable silicon solar cell with high absorption and low transmission and reflection can be achieved when the optimum thickness and base angle of the DLARC are identified. When the thickness of DLARC is varied into a thinner thickness, it can save cost to produce the silicon solar cell that will produce high absorption, low reflection and transmission. This method will be useful for current industrial solar cells.

Anti-reflection coatings are applied to surfaces to prevent light energy from being reflected. An electrical connection to the semiconductor is achieved by making good metal contacts on the n-type and p-type layers. The solar cell is made up of 2 types of semiconductors, p-type and n-type silicon. A solar cell uses the photovoltaic effect to convert light energy into electricity. The photovoltaic effect is caused by the photosynthesis of charge carriers in a light-absorbing material due to the absorption of light radiation. In the case of electron-hole pairs that are formed from the absorption of the photon on the front surface, some are not absorbed but are reflected. There are some methods used to reduce this problem. The front surface of the device can be treated with an anti-reflection coating (ARC) to minimize its reflectance. DLARC can significantly reduce the optical loss of a cell. DLARC's optical properties were quantitatively examined by studying the refractive index of a material. To generate significantly short-circuit current density; the light trapping method is effective for enhancing light absorption. As part of light trapping, multiple light management strategies are used at the same time to achieve 1) Broad light in-coupling at the front side of a (multi-junctional solar cell), 2) Light scattering within the absorber layers and 3) High internal rear reflectance [5,14]. The optimal thickness of DLARC was achieved by combining optical and electrical characteristics. Afterward, the desired solar cell was constructed to

confirm the efficiency simulation design [20]. A quarter wavelength of the DLARC can be used to calculate the thickness of DLARC on the dielectric material to satisfy the quarter-wave condition. For this purpose, the following formula is used:

$$d_1 = \frac{\lambda_c}{4n_1} \quad (1)$$

$$d_2 = \frac{\lambda_c}{4n_2} \quad (2)$$

where  $d_1$  and  $d_2$  are the dielectric material thicknesses followed by the wavelength of the DLARC and  $n_1$  and  $n_2$ . The thickness effects on the electrical and optical properties of the ARC are investigated using the PV Lighthouse Wafer Ray Tracer software. This mathematical technique conducts an optical property of solar cells that are being involved. In the simulation of the software, the changes in reflection, absorption, and transmission of photons can be observed.

Wafer ray tracer simulation is operated by combining a Monte-Carlo algorithm and optical characteristics of selected materials. By considering the absorption parameter and refractive index from the library, the photo generation and optical losses of the constructed device can be calculated. This simulator can help us in finding unexpected results and avoid unnecessary solar design. Wafer ray tracer simulation is a free and open-source simulator and it is user-friendly software without having to write a complicated syntax.

To create a solar cell that can be used, the aim is to solve the issue of optical losses by varying the thickness and base angle of  $\text{Al}_2\text{O}_3$  and ITO.

## Materials and methods

### Simulation procedure

Ray tracing methods are used to calculate the reflection, absorption and transmission of the silicon solar cell. The standard spectrum used is AM 1.5 G that are used to get an integrated irradiance of  $1,000 \text{ W/m}^2$  in the wavelength range from 0 to infinity. The simulation used 5 light trapping schemes that vary the thickness of  $\text{Al}_2\text{O}_3$  and ITO and the angle of the base. The purpose of this simulation was to find the graph of R, A and T; reflection, absorption and transmission of the solar cell. Based on **Table 1**, the material used for the simulation is constant throughout this study. Whereas the thickness of the front film of  $\text{Al}_2\text{O}_3$  and ITO are varied as well as base angle.

**Table 1** The thickness of the material is used as a reference.

	Material	Thickness (nm)
Front film	$\text{Al}_2\text{O}_3$	50 nm
	ITO	70 nm
	a-Si (n)	7 nm
	a-Si: H (i)	5 nm
Substrate	c-Si (n)	160 $\mu\text{m}$
	a-Si: H(i)	5 nm
	a-Si: (p)	7 nm
Rear film	ITO	130 nm

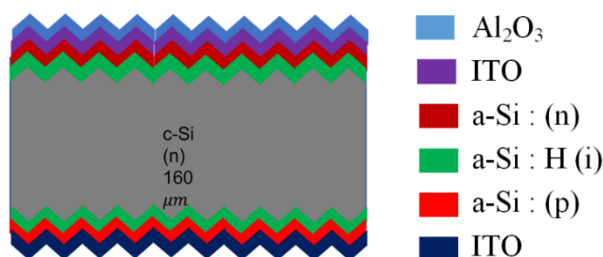


**Figure 1** Model simulation of scheme.

**Table 2** Schemes with different base angles and thickness of ARC.

Light trapping schemes	Height (μm)	Width (μm)	Base angle (°)	The thickness of Al <sub>2</sub> O <sub>3</sub> (nm)	Thickness of ITO (nm)
Reference	3.536	5	54.74	50	70
1	3.536	5	54.74	30	50
2	3.536	5	54.74	15	25
3	3.536	5	70.00	30	50
4	3.536	5	70.00	50	70

## Results and discussion

The results of the 5 schemes are shown in **Figures 2(a) - 2(c)**. Total reflection of the DLARC of the schemes is then discussed (**Figure 2(a)**). The total reflection is analyzed at the wavelength that is 1,200 nm to have a good comparison between all schemes. Scheme 3 has the lowest value of total reflection which is 21 % due to the DLARC used which is Al<sub>2</sub>O<sub>3</sub> and ITO as well as base angle. DLARC minimizes reflectance and improves the overall efficiency of the solar cell [13]. Additionally, compared to SLARC, the cell with DLARC exhibits comparatively low resistance that makes the value of reflection lower in DLARC because more light can be trapped in the solar cell [7]. The results show that DLARC has a greater influence on reducing reflectance within the spectrum range than single-layered ARC and that this impact is highly dependent on altering the film thickness.

The absorption of the DLARC of the schemes is presented in **Figure 2(b)**. The thickness was chosen for the DLARC influencing the absorption of the front film. All 5 schemes have slightly different absorption values due to the thickness chosen as well as the base angle of the scheme that has contributed to that. As shown in **Figure 2(b)**, Schemes 3 and 4 are the best possible scheme for absorption as the value of absorption analyzed is 99 % which are the maximum amount of sunlight that can be absorbed for optimum device performance. High absorption of sunlight in Schemes 3 and 4 was achieved by surface texturing and base angle variation on DLARC thus, increasing the surface area where the absorption of sunlight occurs. In addition, surface texturing in DLARC reduces light reflection, improves light absorption and causes light to bounce back and forth across the surface of the solar cell numerous times [21]. This increases the photoconversion efficiency.

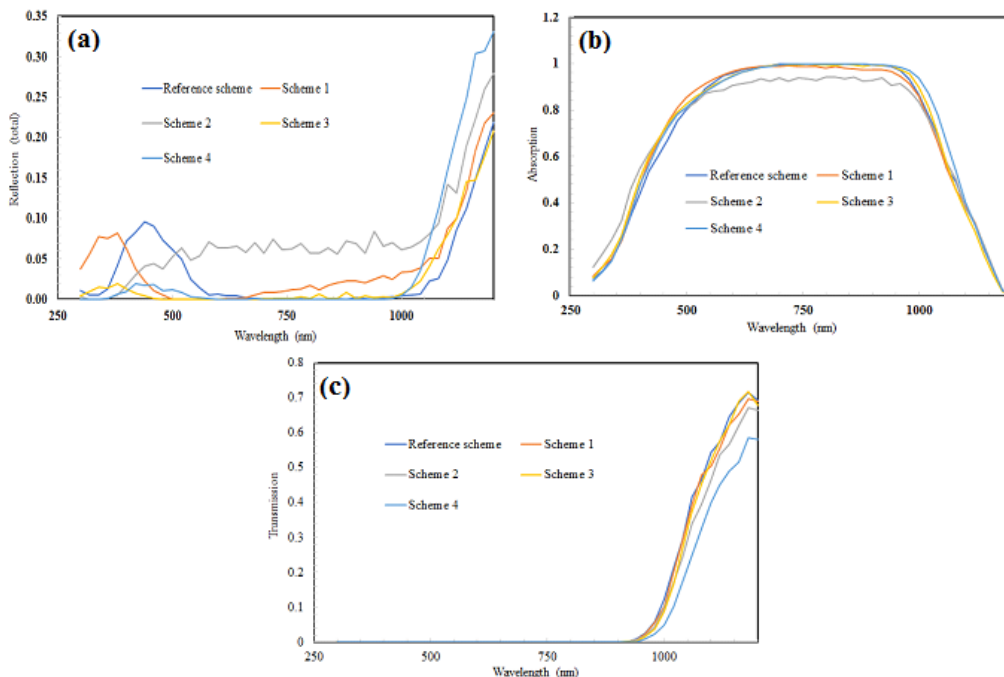


**Figure 2** (a) Reflection, (b) Absorption, and (c) Transmission graphs against wavelength.

The transmission of the DLARC of the schemes is shown in **Figure 2(c)**. We found that the transmission is pretty similar but still can be distinguished at a wavelength of 1,200 nm. Scheme 4 has the lowest transmission among all 5 schemes due to the low value of reflection before. For having DLARC, a lower transmission value makes a higher reflection value and conversely [7]. Besides, Scheme 3 has the lowest value of reflection value, thus having transmission values that are higher than Scheme 4. While Scheme 4 has an increasing value of reflection compared to Scheme 3 but has the lowest value of the transmission. Scheme 4 has the lowest transmission due to a higher value of reflection compared to Scheme 3 due to the light transmitted back on the DLARC. Based on **Figures 2 - 4** and an evaluation of the 5 schemes in **Table 3**, we can conclude that Schemes 1 and 2 shows no improvement with decreasing in the thickness of Al<sub>2</sub>O<sub>3</sub> and ITO layer compared to the reference scheme.

**Table 3** Optical characteristics of all schemes.

Model structure	Reflection (%) (1,200 nm)	Absorption (%) (900 nm)	Transmission (%) (1,200 nm)
Reference height = 3.536 μm width = 5 μm angle = 54.74 ° Thickness Al <sub>2</sub> O <sub>3</sub> = 50 nm Thickness ITO = 70 nm	22	99	69
Scheme 1 height = 3.536 μm width = 5 μm angle = 54.74 ° Thickness Al <sub>2</sub> O <sub>3</sub> = 30 nm Thickness ITO = 50 nm	23	97	69
Scheme 2 height = 3.536 μm width = 5 μm angle = 54.74 ° Thickness Al <sub>2</sub> O <sub>3</sub> = 15 nm Thickness ITO = 25 nm	28	93	66

Model structure	Reflection (%) (1,200 nm)	Absorption (%) (900 nm)	Transmission (%) (1,200 nm)
Scheme 3 height = 3.536 $\mu\text{m}$ width = 5 $\mu\text{m}$ angle = 70.00 $^\circ$ Thickness Al <sub>2</sub> O <sub>3</sub> = 30 nm Thickness ITO = 50 nm	21	99	67
Scheme 4 height = 3.536 $\mu\text{m}$ width = 5 $\mu\text{m}$ angle = 70.00 $^\circ$ Thickness Al <sub>2</sub> O <sub>3</sub> = 50 nm Thickness ITO = 70 nm	33	99	58

Increment from Scheme 1, by increasing the angle of the upright pyramid to 70  $^\circ$  (Scheme 3) shows good improvement in reflection and transmission of the scheme which is 21 and 67 % for reflection and transmission reflectively compared to the reference scheme. Due to this matter, Scheme 3 gives the optimum result of the simulation. Scheme 3 has a low percentage of reflection which is 21 % with high absorption of 99 % which is nearly reaching 100 % results and transmission of 67 %. The device structure of Scheme 3 gives the optimum result when the base angle is changed to 70  $^\circ$  to maximize the absorption of the solar cell. More sunlight can be absorbed due to the base angle changing from 54.74 to 70  $^\circ$  because of the increase in the surface area of the DLARC. The experimental result is based on the reference model structure that has absorption of 99 %, a reflection of 22 %, and transmission of 69 %. When compared with Scheme 3 which gives the optimum result, the value of absorption remains the same whereas the reflection and transmission have been decreasing. The changes of thickness of Al<sub>2</sub>O<sub>3</sub> and ITO to 30 and 50 nm respectively from the reference structure model with a base angle of 70.00  $^\circ$ . With these changes, the value of reflection and transmission has been reduced. A thinner solar cell with high absorption, low reflection and transmission has been achieved with Scheme 3. Using wavelength and absorption from the reference scheme and Schemes 1, 2, 3 and 4,  $J_{\text{max}}$  can be calculated. The graph of EQE against wavelength will then also generate. The photocurrent density,  $J_{\text{max}}$  can be obtained from the R, A, and T graphs by integrating the absorption curve for wavelengths (300 - 1,200 nm) over the AM 1.5 G solar spectrum. The equation is as below:

$$J_{\text{max}} = q \int_{\lambda=300\text{nm}}^{\lambda=1200\text{nm}} EQE(\lambda) \cdot S(\lambda) d\lambda \quad (3)$$

where:

$q$  = electron charge,  $1.6 \times 10^{-19}$  C.

$S(\lambda)$  = the standard spectral photon density of sunlight for the AM1.5G spectrum.

Carrier collection is assumed to be 1 (internal quantum efficiency, IQE = 1) in this calculation. Based on **Table 4**, it is shown that Scheme 3 which has the optimum result has the highest value of  $J_{\text{max}}$  recorded which is 0.3842 mA/cm<sup>2</sup> compared to another scheme. This is due to the thickness of DLARC has been decreasing, together with the base angle that is 70.00  $^\circ$  that has an increase in the surface area making Scheme 3 can minimize the reflection and transmission. The absorption of sunlight in Scheme 3 is also high at 99 %. In this simulation using the Wafer Ray Tracer, the objective has been achieved as the thickness of the DLARC surely gives influences the optical and electrical properties of the solar cell. It can be seen on the value of the  $J_{\text{sc}}$  of Scheme 3 has the highest value which is 0.3842 mA/cm<sup>2</sup>.

**Table 4**  $J_{\text{max}}$  value of the model structure.

Model structure	$J_{\text{max}}$ (mA/cm <sup>2</sup> )
Reference Scheme	0.3819
Scheme 1	0.3828
Scheme 2	0.3671
Scheme 3	0.3842
Scheme 4	0.3826

Due to its employment in several sectors, sodium tungstate ( $\text{Na}_2\text{WO}_4$ ) is a particularly significant tungstate chemical [22]. Huang *et al.* [23], demonstrated that  $\text{Na}_2\text{WO}_4$  has high visible light transparency, flexibility, and stability in addition to demonstrating notable solar thermal-enhanced capacitive performance. Besides, due to their tunable band gap and greater absorption capacity as compared to c-Si, silicon germanium (SiGe) alloys hold significant promise for thin film solar cells [24, 25]. As a result, SiGe and  $\text{Na}_2\text{WO}_4$  have a significant deal of promise for usage in the production of si-based solar cells with high efficiency.

## Conclusions

In conclusion, we have successfully used wafer ray tracer modelling software to simulate the ideal current density of silicon-based solar cells. This paper proposed 4 model structure designs for silicon-based solar cells. As the  $\text{Al}_2\text{O}_3$  and ITO layer thicknesses are reduced in Schemes 1 and 2, there is no improvement over the reference scheme. With Scheme 3, a thinner solar cell with high absorption, low reflection, and transmission has been produced. Due to the light that was reflected back onto the DLARC in Scheme 4, it has a lower transmission than Scheme 3 and a larger value of reflection. We discovered that Scheme 3 had the simulation's best current density, with  $0.3842 \text{ mA/cm}^2$ , compared to the other schemes. Therefore, in order to produce greater current densities in si-based solar cells, the thickness and base angle of  $\text{Al}_2\text{O}_3$  and ITO are crucial.

## References

- [1] Z Zakaria, SK Kamarudin, KAA Wahid and SHA Hassan. The progress of fuel cell for malaysian residential consumption: Energy status and prospects to introduction as a renewable power generation system. *Renew. Sustain. Energ. Rev.* 2021; **144**, 110984.
- [2] S Aftab, MZ Iqbal, Z Haider, MW Iqbal, G Nazir and MA Shehzad. Bulk photovoltaic effect in 2D materials for solar-power harvesting. *Adv. Opt. Mater.* 2022; **10**, 2201288.
- [3] J Qiu, Y Li and Y Jia. *Applications. In: J Leonard (Ed.). Persistent phosphors: From fundamentals to applications.* Woodhead Publishing, Sawston, 2021.
- [4] G Du, Y Bai, J Huang, J Zhang, J Wang, Y Lin, L Lu, L Yang, S Bao, Z Huang, X Chen, M Yin and D Li. Surface passivation of ITO on heterojunction solar cells with enhanced cell performance and module reliability. *ECS J. Solid State Sci. Tech.* 2021; **10**, 035008.
- [5] C Bianchi, AC Marques, RCD Silva, T Calmeiro and I Ferreira. Near infrared photothermoelectric effect in transparent AZO/ITO/Ag/ITO thin films. *Sci. Rep.* 2021; **11**, 24313.
- [6] P Dai, J Long, Q Sun, Y Wu, M Tan and S Lu. Indium tin oxide with high carrier-collection capacity and radiation resistance for GaInP solar cell. *Phys. Status Solidi* 2021; **218**, 2000804.
- [7] MA Zahid, MQ Khokhar, Z Cui, H Park and J Yi. Improved optical and electrical properties for heterojunction solar cell using  $\text{Al}_2\text{O}_3/\text{ITO}$  double-layer anti-reflective coating. *Results Phys.* 2021; **28**, 104640.
- [8] MA Zahid, H Yousuf, Y Kim, EC Cho and J Yi. A novel approach to utilize  $\text{Al}_2\text{O}_3$  and polyolefin encapsulant as an optical and electrical materials to mitigate potential-induced of PV modules. *Opt. Mater.* 2022; **133**, 113022.
- [9] AJ Addie, RA Ismail and MA Mohammed. Amorphous carbon nitride dual-function anti-reflection coating for crystalline silicon solar cells. *Sci. Rep.* 2022; **12**, 9902.
- [10] B Stegemann, J Kegel, M Mews, E Conrad, L Korte, U Sturzebecher and H Angermann. Evolution of the charge carrier lifetime characteristics in crystalline silicon wafers during processing of heterojunction solar cells. *Energ. Procedia* 2014; **55**, 219-28.
- [11] SQ Hussain, S Kim, S Ahn, N Balaji, Y Lee, JH Lee and J Yi. Influence of high work function ITO:Zr films for the barrier height modification in a-Si:H/c-Si heterojunction solar cells. *Sol. Energ. Mater. Sol. Cells* 2014; **122**, 130-5.
- [12] S Tohoda, D Fujishima, A Yano, A Ogane, K Matsuyama, Y Nakamura, N Tokuoka, H Kanno, T Kinoshita, H Sakata, M Taguchi and E Maruyama. Future directions for higher-efficiency HIT solar cells using a Thin Silicon Wafer. *J. Non Crystalline Solid.* 2012; **358**, 2219-22.
- [13] LA Dobrzański, M Szindler, A Drygała and MM Szindler. Silicon solar cells with  $\text{Al}_2\text{O}_3$  antireflection coating. *Cent. Eur. J. Phys.* 2014; **12**, 666-70.
- [14] O Isabella, R Vismara, DNP Linssen, KX Wang, S Fan and M Zeman. Advanced light trapping scheme in decoupled front and rear textured thin-film silicon solar cells. *Sol. Energ.* 2018; **162**, 344-56.

- [15] MA Zahid, MQ Khokhar, S Park, SQ Hussain, Y Kim and J Yi. Influence of Al<sub>2</sub>O<sub>3</sub>/IZO double-layer antireflective coating on the front side of rear emitter silicon heterojunction solar cell. *Vacuum* 2022; **200**, 110967.
- [16] DK Shah, KC Devendra, D Parajuli, MS Akhtar, CY Kim and OB Yang. A computational study of carrier lifetime, doping concentration, and thickness of window layer for GaAs solar cell based on Al<sub>2</sub>O<sub>3</sub> antireflection layer. *Sol. Energ.* 2022; **234**, 330-7.
- [17] W Zhang, K Hu, J Tu, A Aierken, D Xu, G Song, X Sun, L Li, K Chen, D Zhang, P Xu and H Wu. Broadband graded refractive index TiO<sub>2</sub>/Al<sub>2</sub>O<sub>3</sub>/MgF<sub>2</sub> multilayer antireflection coating for high efficiency multi-junction solar cell. *Sol. Energ.* 2021; **217**, 271-9.
- [18] CH Park, JY Kim, SJ Sung, DH Kim and YS Do. Design of grating Al<sub>2</sub>O<sub>3</sub> passivation structure optimized for high-efficiency Cu (In,Ga)Se<sub>2</sub> solar cells. *Sensors* 2021; **21**, 4849.
- [19] IG Kavakli and K Kantarli. Single and double-layer antireflection coatings on silicon. *Turk. J. Phys.* 2002; **26**, 349-54.
- [20] J Houska, J Blazek, J Rezek and S Proksova. Overview of optical properties of Al<sub>2</sub>O<sub>3</sub> films prepared by various techniques. *Thin Solid Films* 2012; **520**, 5405-8.
- [21] KA Salman. Effect of surface texturing processes on the performance of crystalline silicon solar cell. *Sol. Energ.* 2017; **147**, 228-31.
- [22] F Dkhilalli, S Megdiche, K Guidara, M Rasheed, R Barillé and M Megdiche. AC conductivity evolution in bulk and grain boundary response of sodium tungstate Na<sub>2</sub>WO<sub>4</sub>. *Ionics* 2018; **24**, 169-80.
- [23] WM Huang, CY Hsu and DH Chen. Sodium tungsten oxide nanowires-based all-solid-state flexible transparent supercapacitors with solar thermal enhanced performance. *Chem. Eng. J.* 2022; **431**, 134086.
- [24] E Kadri, M Krichen, R Mohammed, A Zouari and K Khirouni. Electrical transport mechanisms in amorphous silicon/crystalline silicon germanium heterojunction solar cell: Impact of passivation layer in conversion efficiency. *Opt. Quant. Electron.* 2016; **48**, 546.
- [25] E Kadri, K Dhahri, R Barillé and M Rasheed. Novel method for the determination of the optical conductivity and dielectric constant of SiGe thin films using Kato-Adachi dispersion model. *Phase Transit. A Multinational J.* 2021; **94**, 65-76.